

Fermi National Accelerator Laboratory

FERMILAB-Pub-84/97-E
7000.723
UR-898

SEARCH FOR ANOMALOUS GRAVITATIONAL EFFECTS
AT THE FERMILAB ACCELERATOR

Progress Report on E-723

P. Reiner, J. Rogers, W. Wuensch, and A. C. Melissinos
University of Rochester, Rochester, New York 14627

and

W. B. Fowler and M. Kuchnir
Fermi National Accelerator Laboratory, Batavia, Illinois 60510

October 1984

Search for anomalous gravitational effects
at the Fermilab accelerator

- Progress Report on E-723 -

P. Reiner, J. Rogers, W. Wuensch, and A. C. Melissinos

Department of Physics and Astronomy

University of Rochester, Rochester, NY 14627

W. B. Fowler and M. Kuchnir

Fermilab, Batavia, IL 60510

Abstract

We report on the results of tests of a gravitational detector operated in the CØ area of the Fermilab accelerator in June and July of this year. Our experience so far is that these measurements are feasible and we have set a limit on the ratio of the coupling of a long range force to that of the gravitational constant of $g/G < 3 \times 10^{20}$. The sensitivity of the experiment is evaluated to be 0.5×10^6 times lower than for the test-run and should be achieved during the forthcoming fixed target operating period.

1. Introduction

The circulating beam of a high energy accelerator provides a unique opportunity for measuring the gravitational interaction at high relative velocity. As is well known the gravitational potential of a body of mass m moving with velocity $v \rightarrow c$ can be calculated from Einstein's theory and is given by (1,2)

$$h^{\circ \circ} = \frac{2mG}{c^2(b^2 + \gamma^2 v^2 t^2)^{\frac{1}{2}}} [2\gamma^2 \beta^2 + 1] \quad (1)$$

where b is the distance of closest approach, which takes place at $t=0$.

From the potential one obtains the acceleration felt by a stationary observer. The average transverse acceleration for a single bunch of N particles circulating with a period τ_0 is attractive and given by

$$\langle a \rangle = \frac{1}{\tau_0} \frac{2NmG}{\gamma \beta c} \frac{1}{b} [2\gamma^2 \beta^2 + 1] \quad (2)$$

The energy dependence of Eqs (1,2) is a direct measure of the tensor nature of gravitation, and is absent in a vector theory.

To observe an effect one takes advantage of the periodicity of the signal and uses a resonant detector. One approach is based on mechanically resonant detectors where the endwall reaches a (maximal) harmonic displacement

$$\delta x = \langle a \rangle Q_m / \Omega^2 \quad (3a)$$

after time

$$\delta t = Q_m / \Omega \quad (3b)$$

Alternately one makes a direct measurement of the potential $h^{\mu\nu}$ by exploiting its coupling to the electromagnetic field. The corresponding "equivalent" displacement is

$$\delta x = \langle h \rangle L \quad (4)$$

where L is the length of the detector. The two effects have different

origin in that the result of Eqs (3) is due to the gradient of $h^{\mu\nu}$ whereas that of Eq (4) is a result of the change of the metric.

Since we are using tuned detectors only the appropriate Fourier component of the beam distribution contributes. This is implied in the expressions for the average $\langle a \rangle$ or $\langle h \rangle$ in the above equations. The data discussed here were obtained during acceleration and flat top (~40 sec) with a beam intensity of 7×10^{12} protons per cycle. The frequency of the detector was at the 26th harmonic of the fundamental

$$\Omega/2\pi = 1.240541 \text{ MHz} \quad (5).$$

The Fourier component at that harmonic was measured (in agreement with calculation) to be -20 db as compared to the maximum effect. The detector was placed at a distance of $b=760$ cm from the beam. One obtains

$$\langle a \rangle = 1.2 \times 10^{-25} \text{ cm/sec}^2 \quad (6a)$$

$$\langle h \rangle = 10^{-42} \quad (6b)$$

Using an equivalent mechanical $Q_m = 2.8 \times 10^3$

$$\delta x = 6 \times 10^{-36} \text{ cm} \quad (6c)$$

It is clear that the acceleration of a resonant mass has greater sensitivity than the coupling due to the change in metric. In particular at low frequency and for high mechanical Q_m the sensitivity can be greatly improved and is only limited by the thermal noise in the detector. However there is a limit on Q_m from the available coherence time δt . At present $\delta t = 10$ sec but in a stored beam operation $\delta t \sim 10^3$ sec can be easily realized. Thus at the fundamental frequency one can use $Q_m = 10^8$, a value that has been reached for bar detectors. On the other hand the coupling through the change in metric is independent of frequency and the detector will respond to any perturbation that couples to the energy of the electromagnetic field in the cavity. Therefore the experiment places limits on possible long-range forces that exhibit such a direct coupling.

As an example, a light mass axion field would mediate such an interaction⁽³⁾.

If we express the coupling of the unknown interaction by g , and the gravitational constant by G , the present test establishes

$$g/G < 3 \times 10^{20} \quad (7a)$$

and in the forthcoming run we expect to reach

$$g/G < 6 \times 10^{14} \quad (7b)$$

For comparison we note that $G_F/G \sim 10^{28}$ and $\alpha/(Gm_p^2) \sim 10^{36}$. In establishing these limits we have used the sensitivity given by Eq.(6c) and therefore the limits are dependent on a precise measurement of Q_m .

2. The Detector

The detector is a microwave parametric converter operating at 10 GHz. It consists of two coupled superconducting cavities so as to form a two-level system, the level spacing being set equal to the frequency of the perturbation. When the em field stored in the cavity is perturbed at its resonant frequency by a fractional change h , transitions occur to the second level and the power that can be measured at that level is

$$P_2 = P_1 (hQ)^2 \quad (8)$$

Here Q is the loaded electrical quality factor; unloaded Q -values of $Q_0 \sim 3 \times 10^8$ have been obtained at $T=1.6^\circ$ K. The perturbation expressed by the dimensionless parameter h could represent endwall motion, $h=\delta x/L$ with $L \sim 10$ cm typical of the dimensions of the cavity; or the change in the metric. More details can be found in references (4,5).

The detector was installed in the CØ spectrometer room as shown in Fig. 1, at a distance ~ 7.6 m from the beam. The detector frequency was tuned to the 26th harmonic [see Eq (5)] and its output was compared with a reference signal derived from the beam circulation frequency. This was achieved by using a signal from the master frequency oscillator and

multiplying it up to the 26th harmonic. Furthermore the stability of the reference was checked by comparing it to the direct signal from the beam pick-ups at CØ.

Comparison of the two frequencies makes it possible to use narrow detection bandwidth, $BW = 0.025$ Hz, with a consequent decrease in noise. The detection scheme is shown in Fig. 2. We use a pair of coupled synthesizers which are offset by 7 Hz to mix the 1.2 MHz signals to 114 KHz. These signals are then amplified and mixed in a PAR lock-in detector producing a 7 Hz signal which is detected by an FFT.

We made measurements from injection into the Saver until the end of flat top, or in subsets of this interval. During acceleration (from 150 + 800 GeV) the change in β and thus also frequency is

$$\Delta\beta/\beta = 1.886 \times 10^{-5} \quad (9)$$

which corresponds at the 26th harmonic to

$$\delta f = 23.4 \text{ Hz.}$$

Of course we are tracking this frequency change in the detection scheme. However it must remain within the width of the levels; this is possible because for $Q = 3 \times 10^8$, the level width is $\Delta f_d \approx 30$ Hz.

The calibration and tuning of the detector was accomplished by using the reference frequency to drive a piezoelectric crystal (PZT) placed on the cavity endwall. The resulting signal is shown in Fig. 3a where it is 50 db above noise level. The square of the PZT drive amplitude is plotted vs P_2 in Fig. 3b, indicating that the detector obeys Eq (8). If the detector frequency was not properly set no conversion could be observed. To set the difference frequency the dimensions of one of the cavities are mechanically changed; this affects f_1 and thus Δf according to

$$\Delta f = \sqrt{(f_1 - f_2)^2 + K^2 f_1 f_2} \quad (10)$$

where $Kf = \Delta f_{\min}$ is the minimum separation which is fixed by the coupling aperture.

3. The Frequency Spectrum of the Saver

Originally we contemplated doing the experiment with the beam in stored mode. Because, however, of the availability of time during fixed target running we have examined the frequency spectrum in the Saver during normal operation at 800 GeV. This was accomplished by using the beam pick-ups mixing down the signals and then Fourier analyzing on the FFT.

The dominant frequency component is of course the 53 MHz due to the structure of the buckets. An example of the measurement of this frequency is given in Fig. 4a where the abscissa spans the last 2 KHz. The traces are taken at intervals of 1/3 sec and one can see the injection porch, the change in β during acceleration and the flat-top region. From Eq.(9) one expects a frequency change of 1002 Hz whereas from the frequency analysis (see Fig. 4a) we obtain 1001 ± 2 Hz. Note that a 10 Hz change in frequency corresponds to a change in radius of 0.2 mm. Fig. 4b shows the magnet ramp equivalent to this acceleration process.

The Saver operates with one empty booster batch and there are several (2 to 5) empty buckets between batches. This structure as well as the inhomogeneities from batch to batch and between buckets give rise to a spectrum of harmonics. In Fig. 5a we show the power in the lower harmonics as measured (solid line). The dashed line gives the results of a very simplified model calculation. One notes the prominence of the 13th harmonic and its multiples which is due to the empty buckets between batches. The power levels are referenced to 0 db at 53 MHz. The higher harmonics are shown in Fig. 5b and their distribution reflects the width of the buckets which is typically 2 nsec. The graph of Fig. 5b which was obtained during low β tests is not a completely true representation of the

beam because of the bipolar output of the pickups. Many low level sidebands are also present in the spectrum but are not apparent in the figure.

From this analysis we conclude that the effective beam intensity contributing at the 26th harmonic is 10^{-2} of the full beam. We use this figure in estimating the limits of the coupling of the beam to the detector.

4. Results

The data was integrated during every acceleration cycle and the resulting frequency spectrum written on tape via the PDP-11. The integration time of $\delta t = 40$ sec sets the limit of the bandwidth resolution at $BW = 25 \times 10^{-3}$ Hz. A typical spectrum is shown in Fig. 6a and spans 10 Hz (there are 401 channels in the FFT). As explained before the signal is expected at 7 Hz. Several of these spectra are then averaged off-line. The result for 367 averages (-7 hours of data) is shown in Fig. 6b.

In this averaging process, the phase information is not available so that the noise fluctuations decrease only as $1/\sqrt{N}$. Since the bandwidth is not changed the noise floor remains the same. From Figs. 6 the noise level at 7 Hz - the expected position of the signal - is $S_N = -65$ dBV. We translate this to power at the cavity by accounting for gain in the amplifiers and losses in the mixers and transmission lines

(10 GHz ampl.)	= + 42 db	(Mixers)	- 11 db
(IF ampl.)	= + 29.8 db	(Transmission)	- 2 db
(Lock-in)	= + 72 db	(Attenuator)	- 12 db

Indicating a net gain of 118.8 db. The input to the FFT is at 50 Ω (dbm = dbV + 13) so that the observed signal corresponds to -170.8 dbm at the cavity or

$$P_2 = 0.81 \times 10^{-20} \text{ W} \quad (11)$$

in bandwidth $B = 25 \times 10^{-3} \text{ Hz}$

The input power in this case was $P_1 = 40 \text{ mW}$ and the electrical loaded $Q = 1.42 \times 10^7$ because the detector was operated at $T = 4.2^\circ \text{ K}$. The cavities were critically coupled so that we obtain⁽⁵⁾

$$\Delta x = (27.3 \text{ cm}) \left[\frac{P_2}{P_1} \frac{4}{Q^2} \right]^{\frac{1}{2}} = 1.7 \times 10^{-15} \text{ cm} \quad (12)$$

The factor of 27.3 cm is larger than the dimensions of the cavity ($l \sim 10 \text{ cm}$) and has been established experimentally.⁽⁵⁾ Comparing this result with the expected effect as given by Eq. (6c) we obtain the limit indicated in Eq. (7a): $g/G < 10^{19}$.

The power level given in Eq. (11) can be expressed as a noise equivalent temperature at the input of our system according to

$$P_2 = 4 k T_e B \quad (13)$$

which yields $T_e = 5,600^\circ \text{ K}$. The noise equivalent temperature of the microwave amplifier has been measured⁽⁶⁾ to be $T_{ne} = 650$; thus further improvement can be expected in the level of minimum detectable power.

The expected signal can be simulated by allowing pick-up of the reference frequency in the signal line before mixing down. By appropriate shielding and isolation we have reduced this effect below the noise level; as in Figs 6. However when the microwaves become unlocked the microwave amplifier is saturated. As a result 40 db of gain are lost and the noise level drops as shown in Figs 7a,b. Here the noise level at 7 Hz is -80 dbV which would be equivalent to an input $T_e = 250$ which is not possible if the

microwave amplifier was functioning properly. Thus the observed signals in these figures are spurious and are due to pick-up. They do however simulate the expected signal (this is the analogue of Monte Carlo results in a particle physics experiment). Note that the pick-up level, in both the 30 averages plot (Fig. 7a) and in the 454 averages plot (Fig. 7b) does not exceed ≈ 68 dBV, that is, it is below the noise floor of the data shown in Fig. 6 which was used to establish the results of this test.

5. Expected Improvements and Discussion

The expected improvements arise from:

- (a) Decrease the separation between the detector and the beam which gives a factor $R_a = 25$
- (b) Increase in input power to $P_1 = 7W$, as well as improvement in minimum detectable signal to $P_2 = 4 \times 10^{-22}$. This results in a gain in sensitivity by a factor of $R_p = (3500)^{1/2} \approx 60$
- (c) Increase in the electrical Q by lowering the cryostat temperature (pumping) to 1.2° K, which yields $R_q = 30$.

The aggregate of these improvements should allow us to reach

$$g/G < 7 \times 10^{15} \quad (14)$$

The above limit is based on a signal/noise ratio of one in the 25 MHz bandwidth. With longer integration time one will be able to gain in principle another factor of 10 if the effective bandwidth can be reduced to 0.25 MHz. Finally it is possible to gain a factor in effective beam intensity by operating the accelerator with ~ 20 empty buckets between batches, yielding a 5-fold improvement in sensitivity. Therefore, under normal accelerator operations one can reach the limit of Eq.(7b). With special operation it should be possible to exceed $g/G < 10^{14}$.

The identification of spurious signals is most effectively achieved by changing the Q of the detector through the control of the temperature. The

available range in Q is a factor of 30, so that the power level of a genuine signal should change by a factor of 10^3 . On the other, hand pick-up should not be affected by temperature changes.

So far we have not observed an effect of the beam, such as could be expected from particle spray or from the direct em coupling. These effects will become much more important now that the detector is in the tunnel and in close proximity to the beam pipe. The experience on the absence of these effects so far is encouraging.

6. Acknowledgements

This work would not have been possible without the assistance and support of many persons in particular at Fermilab. They are too numerous to name individually here but we are particularly indebted to P. Limon, J. R. Orr, T. Toohig, F. Turkot and R. Vanacek of the Accelerator division; to A. McInturf and H. Warren for the use of Lab II. The support of this experiment by the Fermilab Physics department and by the Research division has been essential and is sincerely acknowledged. Special thanks are due to D. Ritchie and his group for computing support and to B. Brown, H. Jöstlein and R. Pasquinelli for their continued advice and interest in this project.

References and Notes

- (1) A. C. Melissinos, *Il Nuovo Cimento* 62B, 190 (1981).
- (2) V. B. Braginsky, C. M. Caves and K. S. Thorne, *Phys. Rev.* D15, 2047 (1977).
- (3) See for instance J. E. Moody and Frank Wilczek, *Phys. Rev.* D30, 130 (1984).
- (4) C. E. Reece et al., *Physics Letters A* (1984) in press. See also C. E. Reece, P. J. Reiner and A. C. Melissinos, "A detector for high frequency gravitational effects based on parametric conversion at 10 GHz", *Proceedings of the 1982 Snowmass Meeting of the DPF*, p. 394.
- (5) C. E. Reece, "A superconducting microwave cavity parametric converter transducer sensitive to 10^{-19} m harmonic motion", Ph.D. thesis University of Rochester Report UR-867 (unpublished).
- (6) J. T. Rogers, "Measurement of Johnson and amplifier noise at 10 GHz", University of Rochester Report UR-873 (unpublished).

Figure Captions

- Fig. 1 Experimental layout in the CØ area.
- Fig. 2 Schematic of detection electronics.
- Fig. 3 Calibration of the detector using the beam circulation signal. (a) Response of the FFT to a 1 V signal. (b) Upconverted power vs the square of the PZT driving voltage.
- Fig. 4 Variation of the 1113th harmonic during acceleration from 150 to 800 GeV in the Saver. (a) Frequency measurements made at 1/3 sec intervals; the total change in frequency is $\Delta f = 1001$ Hz out of 53.104 MHz. (b) The magnet ramp during acceleration.
- Fig. 5 The frequency spectrum of the Saver. (a) The lower harmonics $n = 1$ to 30 on a logarithmic scale. (b) The higher harmonics appear at multiples of the R.F. frequency.
- Fig. 6 The detector output signal shown as a 400 channel frequency spectrum spanning 0 to 10 Hz. The signal is expected at 7 Hz as shown in Fig. 3a. (a) Average of 17 spectra. (b) Average of 367 spectra.
- Fig. 7 Simulation of expected signal obtained by allowing pick-up into the final detection stage. (a) Average of 30 spectra. (b) Average of 454 spectra.

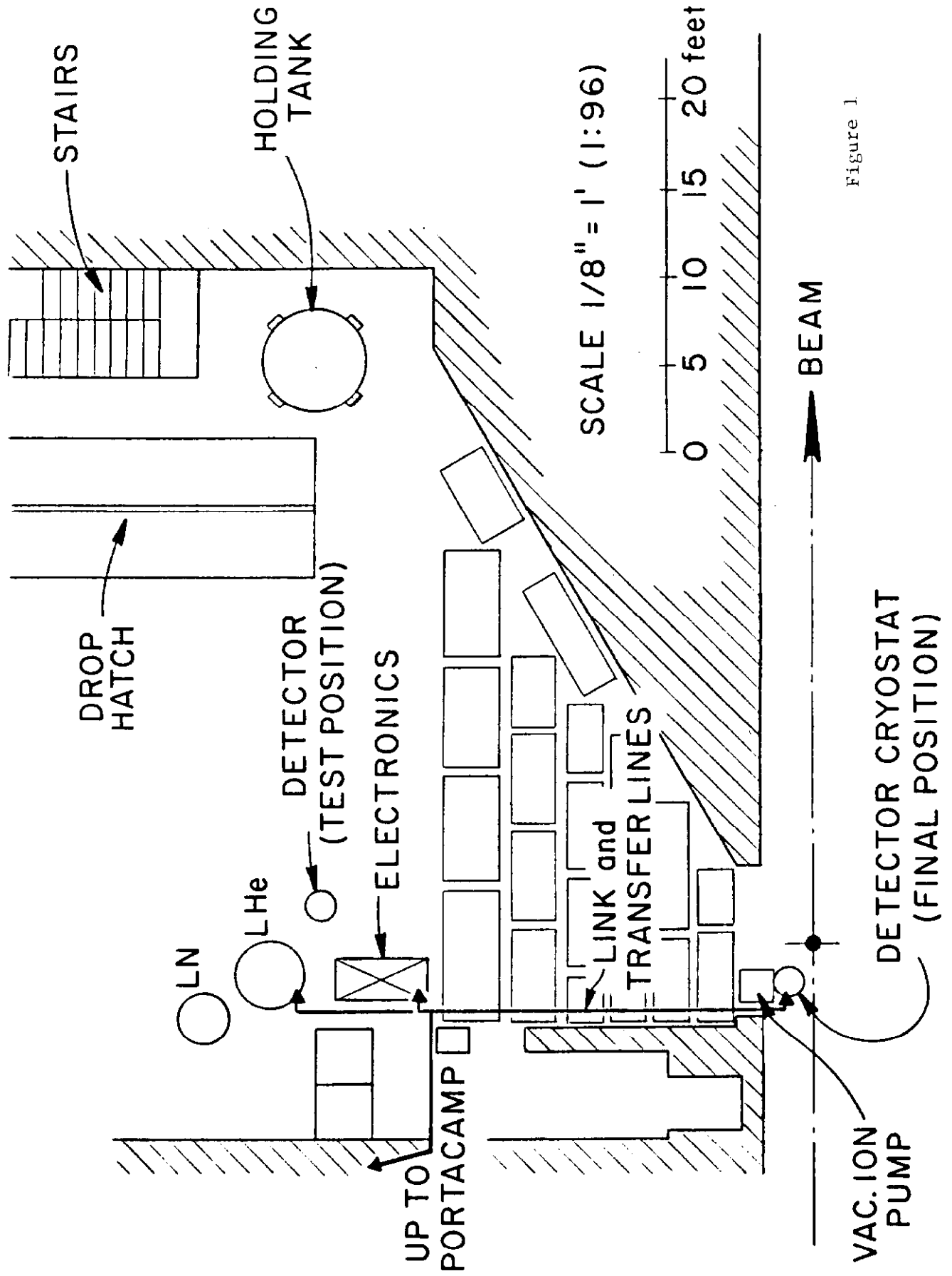
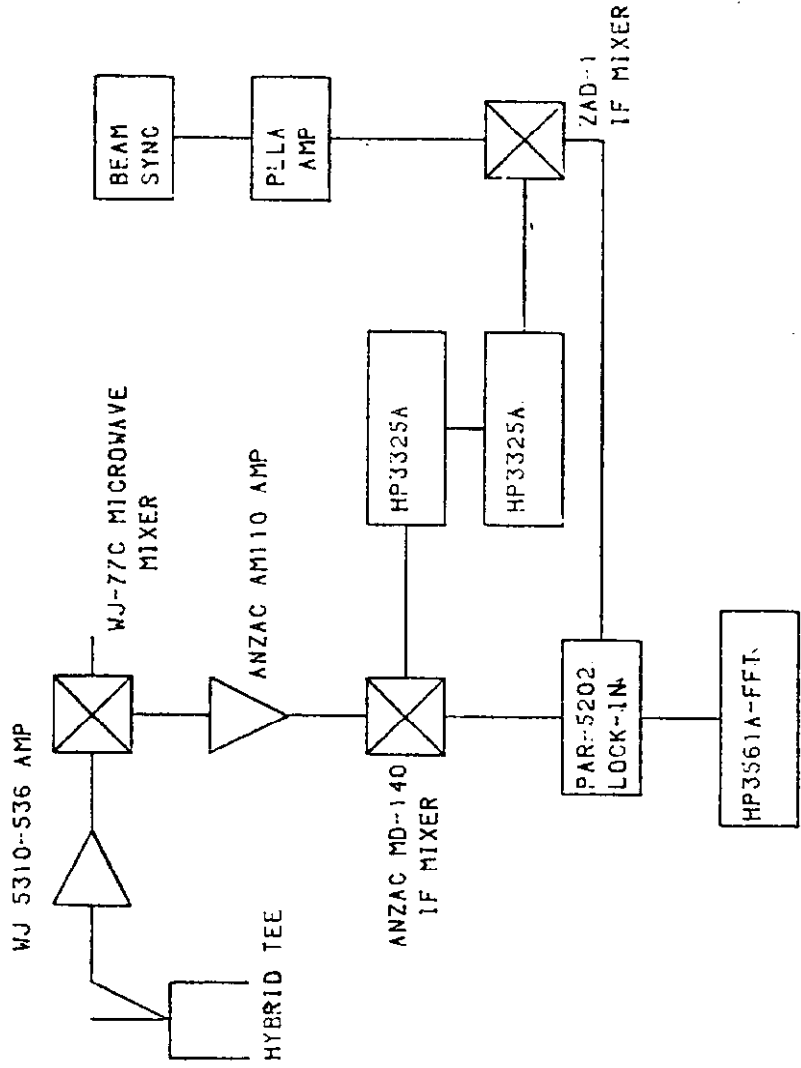


Figure 1



TWO MIXER MODE DETECTION SYSTEM

Figure 2

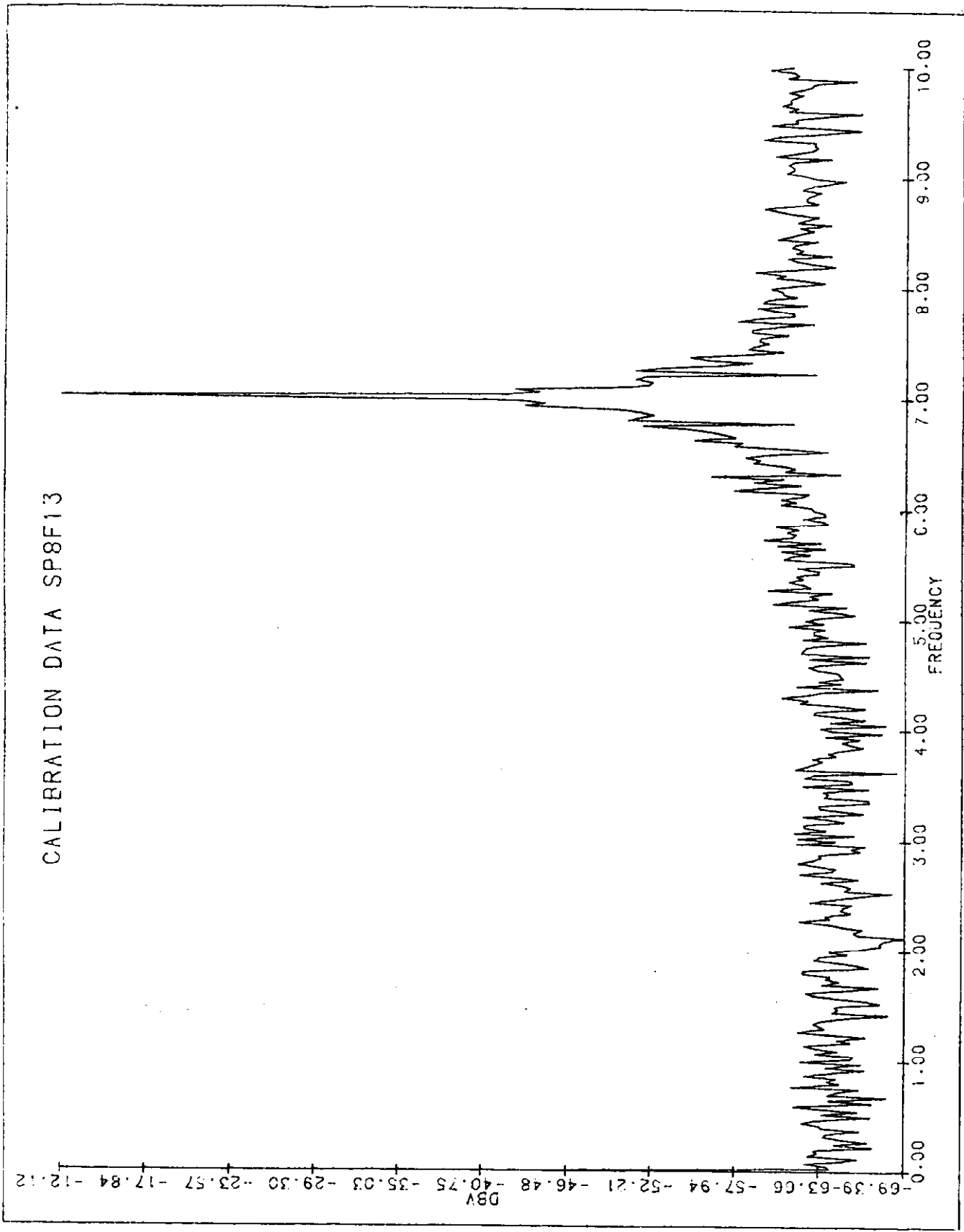


Figure 3a

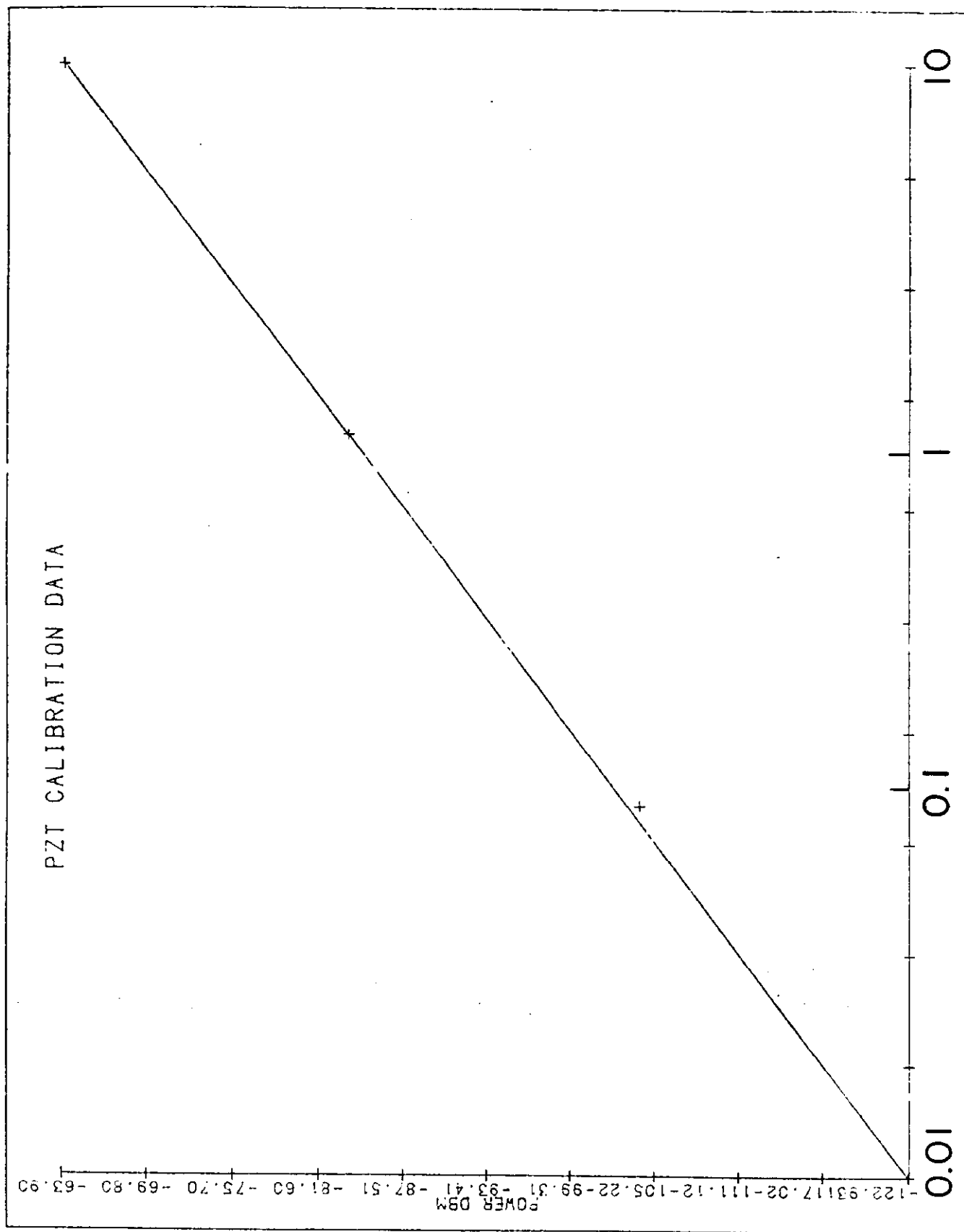
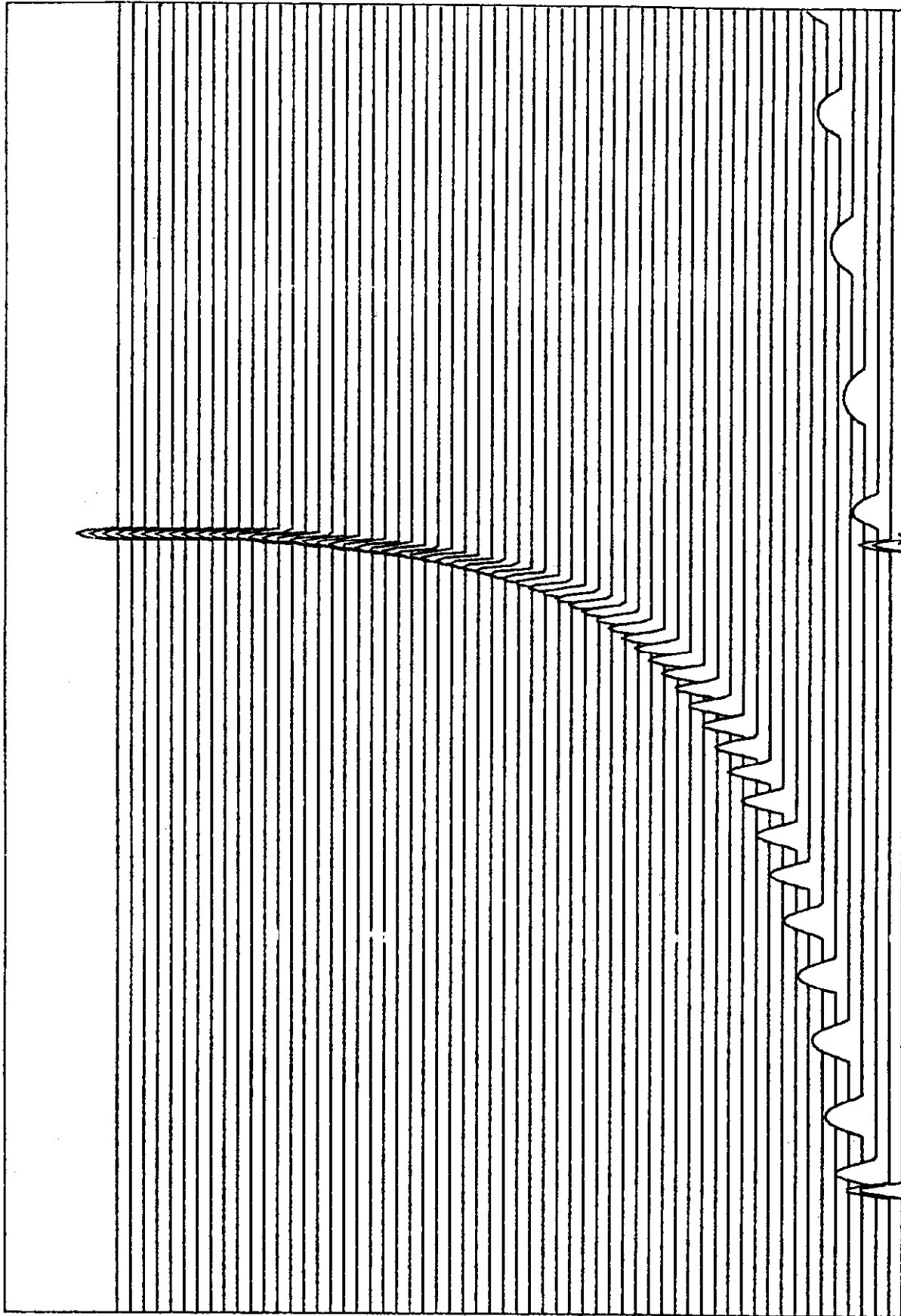


Figure 3b

RANGE: -41 dBV STATUS: PAUSED

1/60 A: MAG

0
dBV



10
dB
/DIV

-80

START: 800 Hz

X: 1995 Hz

BW: 7.5 Hz

Y: -98.49 dBV

STOP: 2800 Hz

Figure 4a

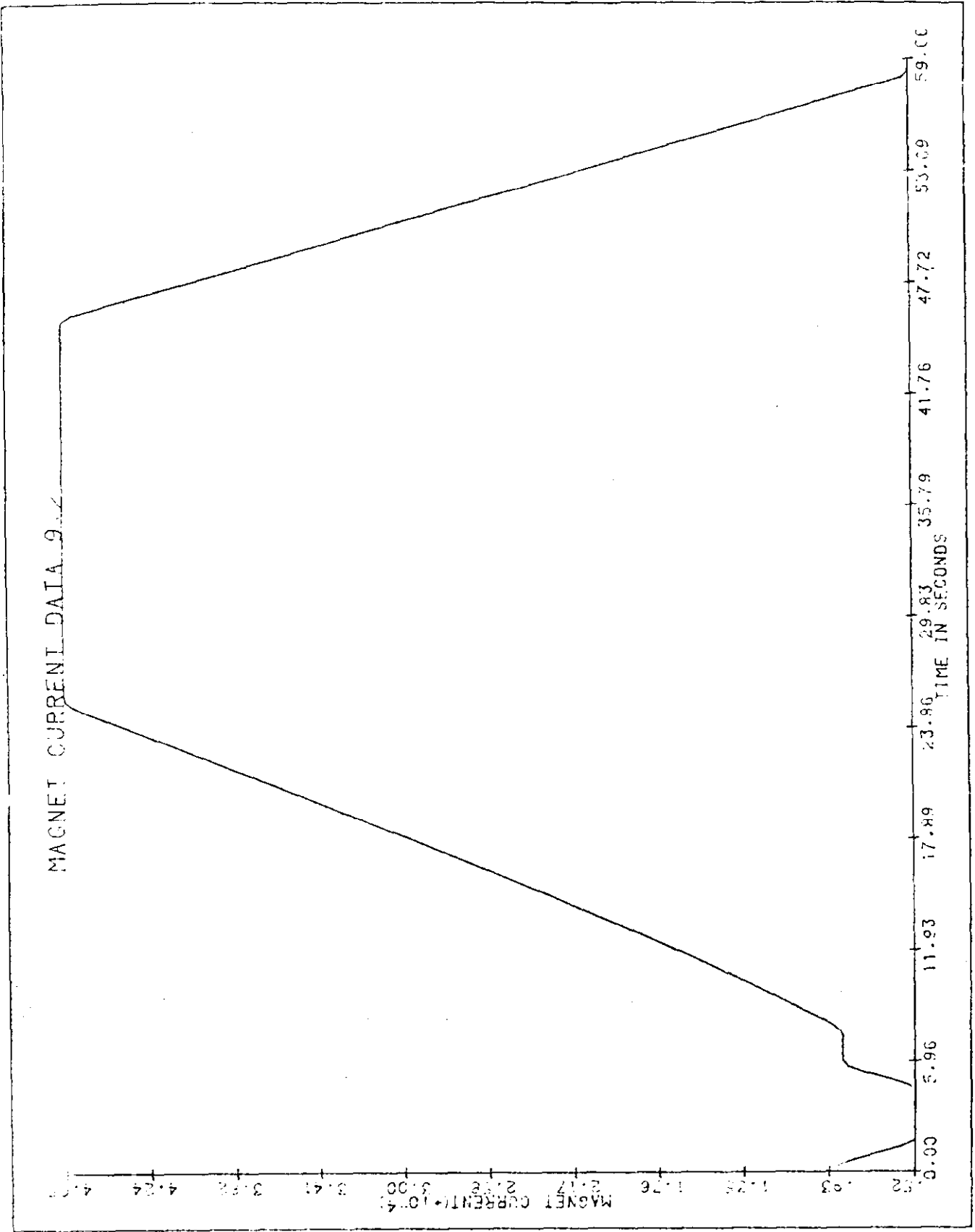


Figure 4b

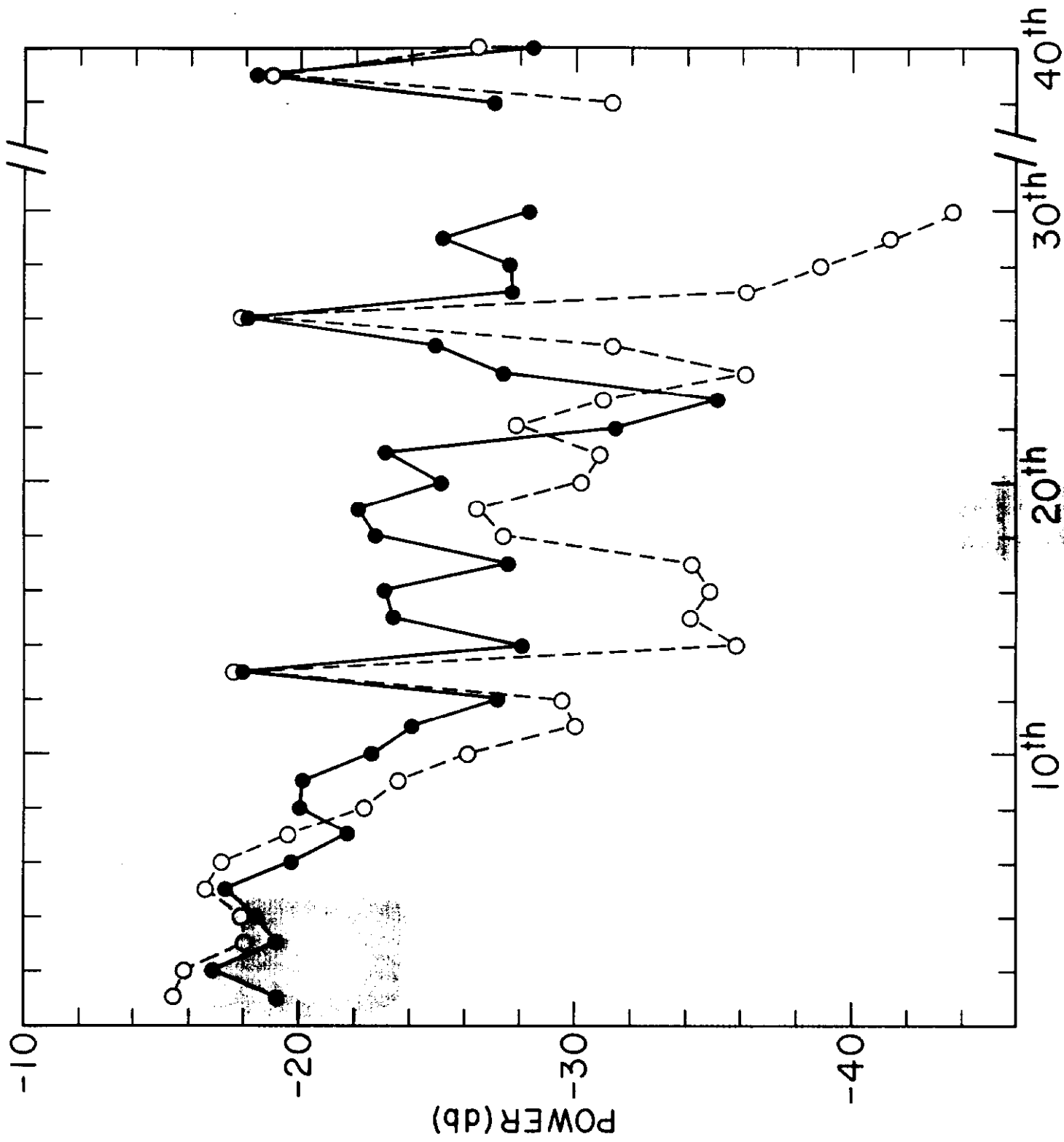


Figure 5a

TEV I FREQUENCY SPECTRUM

5/9/84 LOW β TESTS

BUCKET SIZE ~ 2 nsec

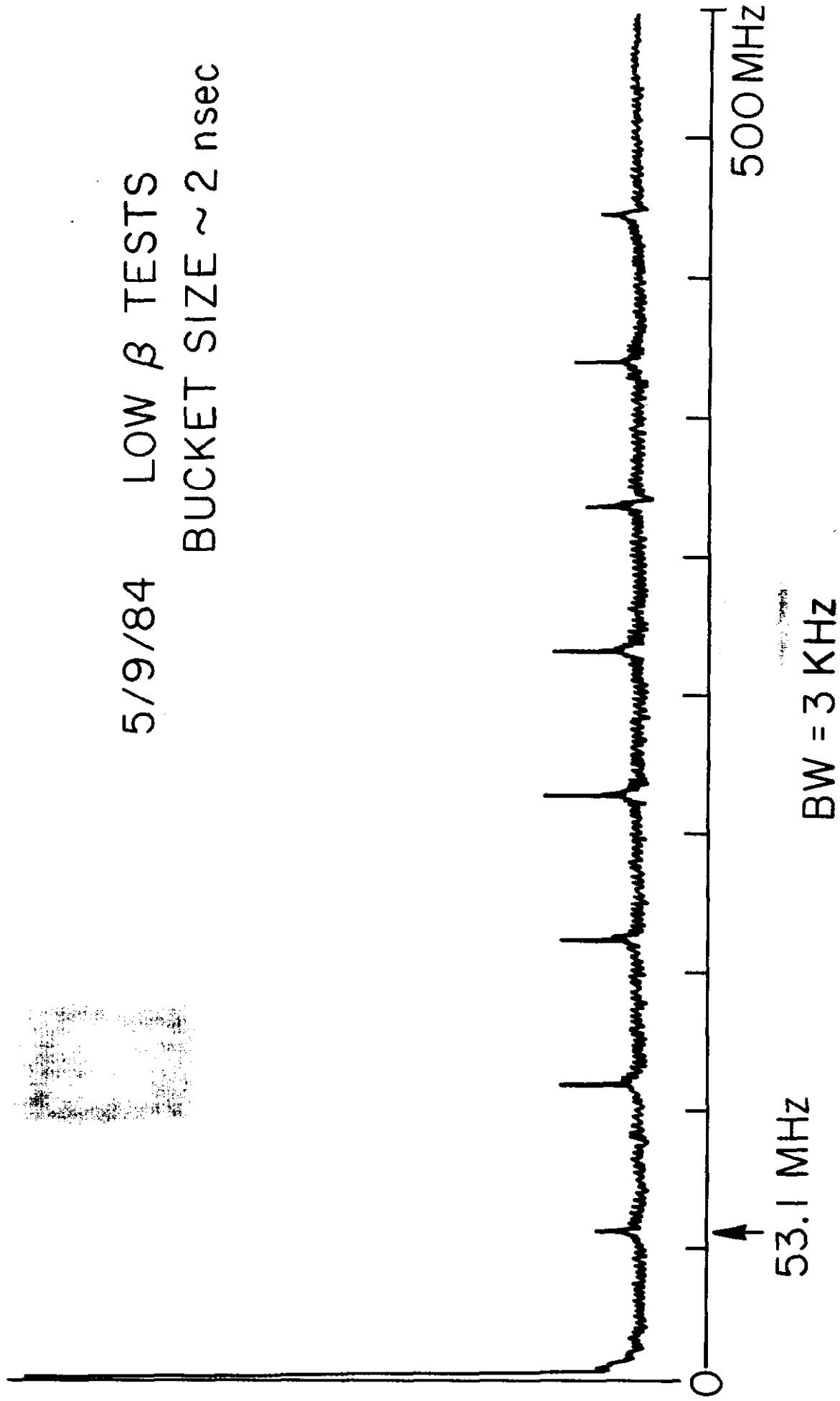


Figure 5b

UPCONVERSION DATA SP8F14

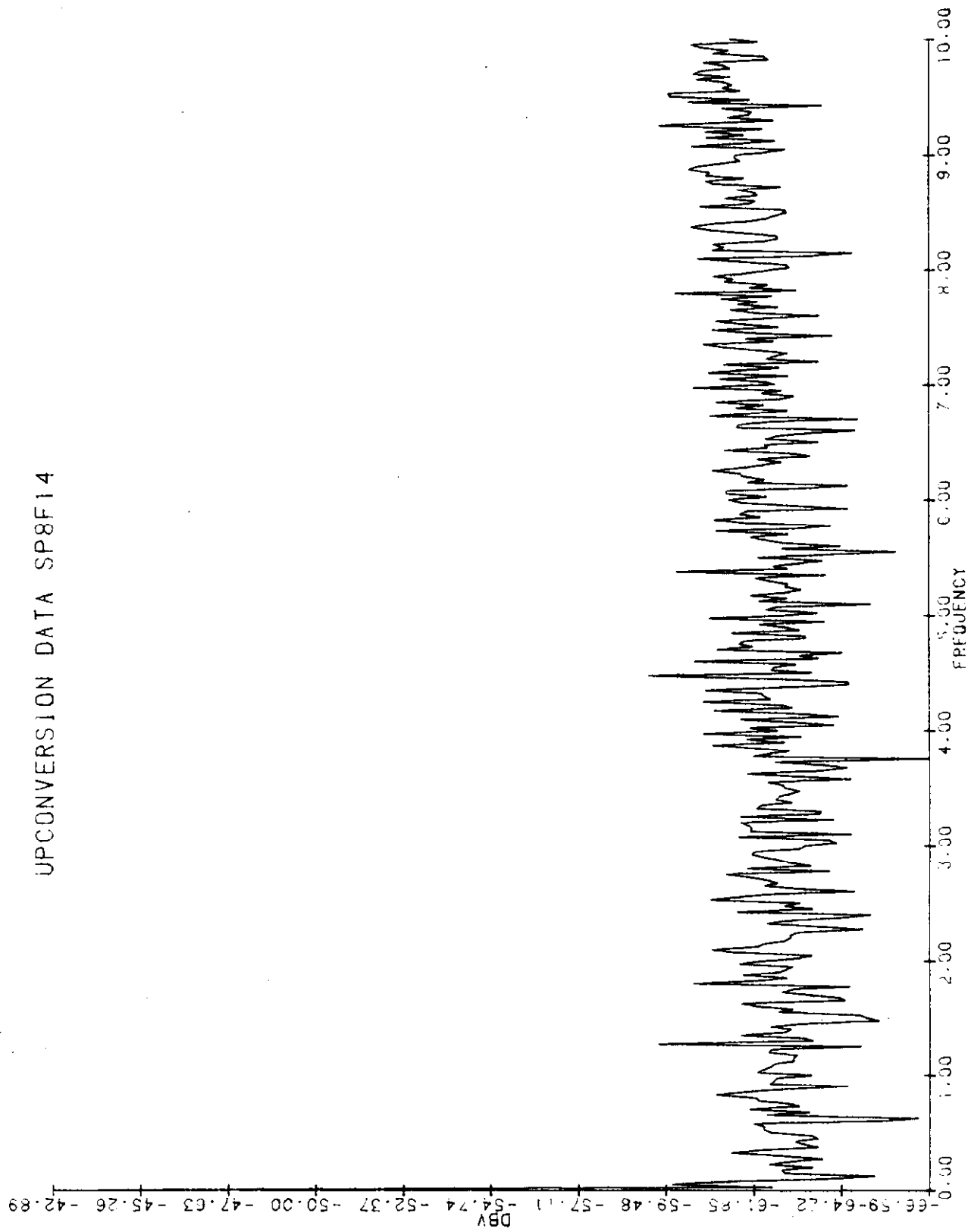


Figure 6a

UPCONVERSION DATA AVEDAT1

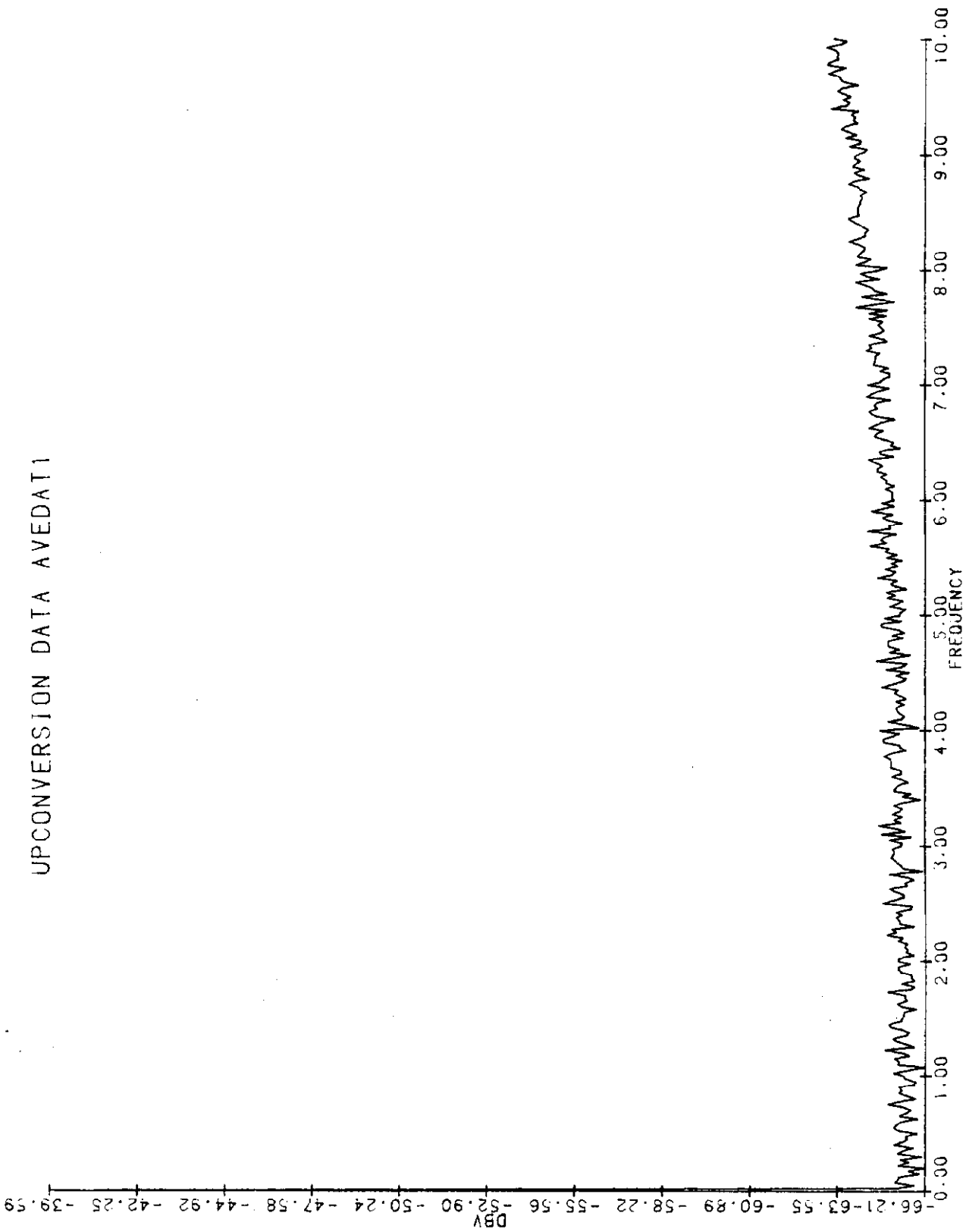


Figure 6b

UPCON. DATA CUT ON 10.3

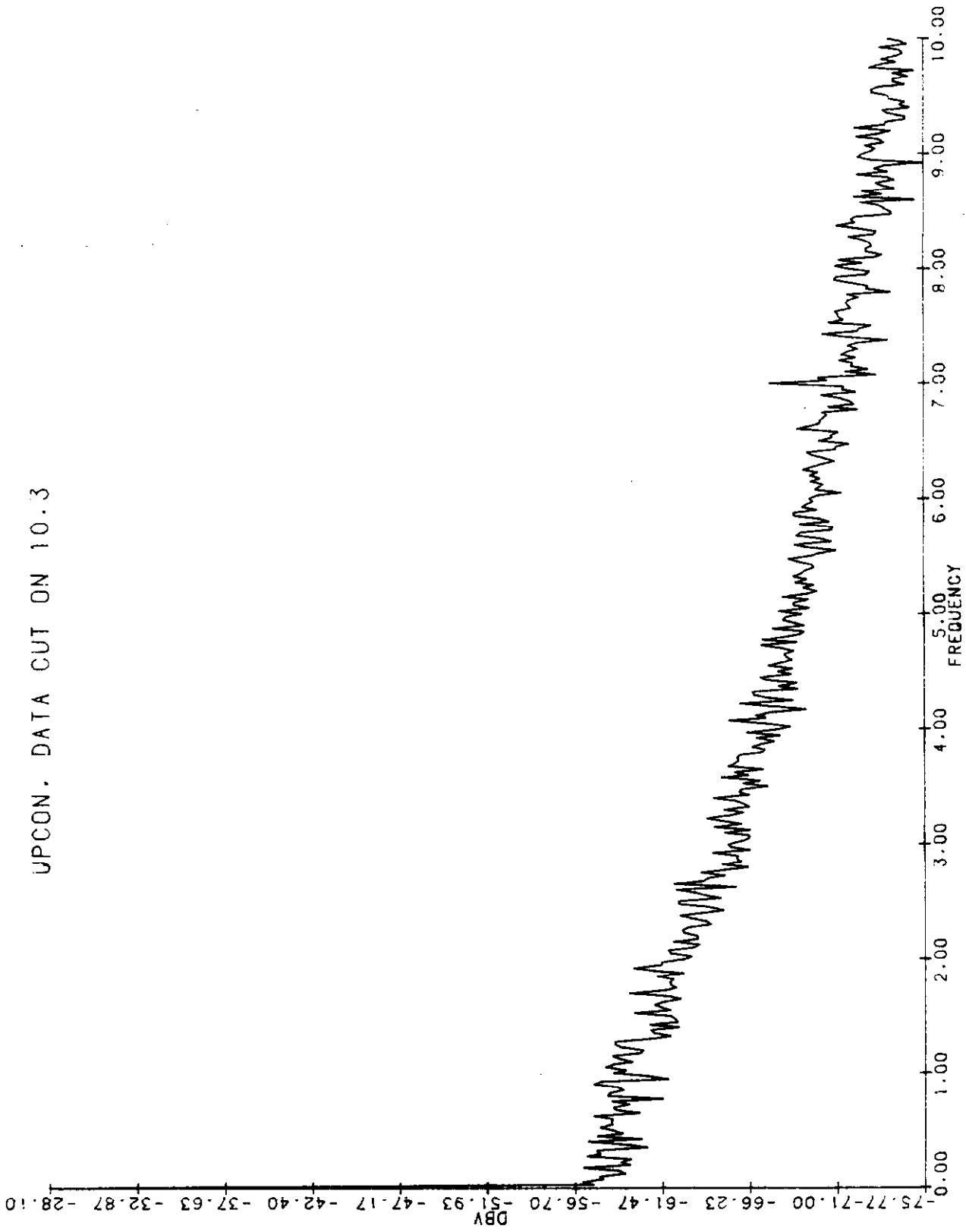


Figure 7a

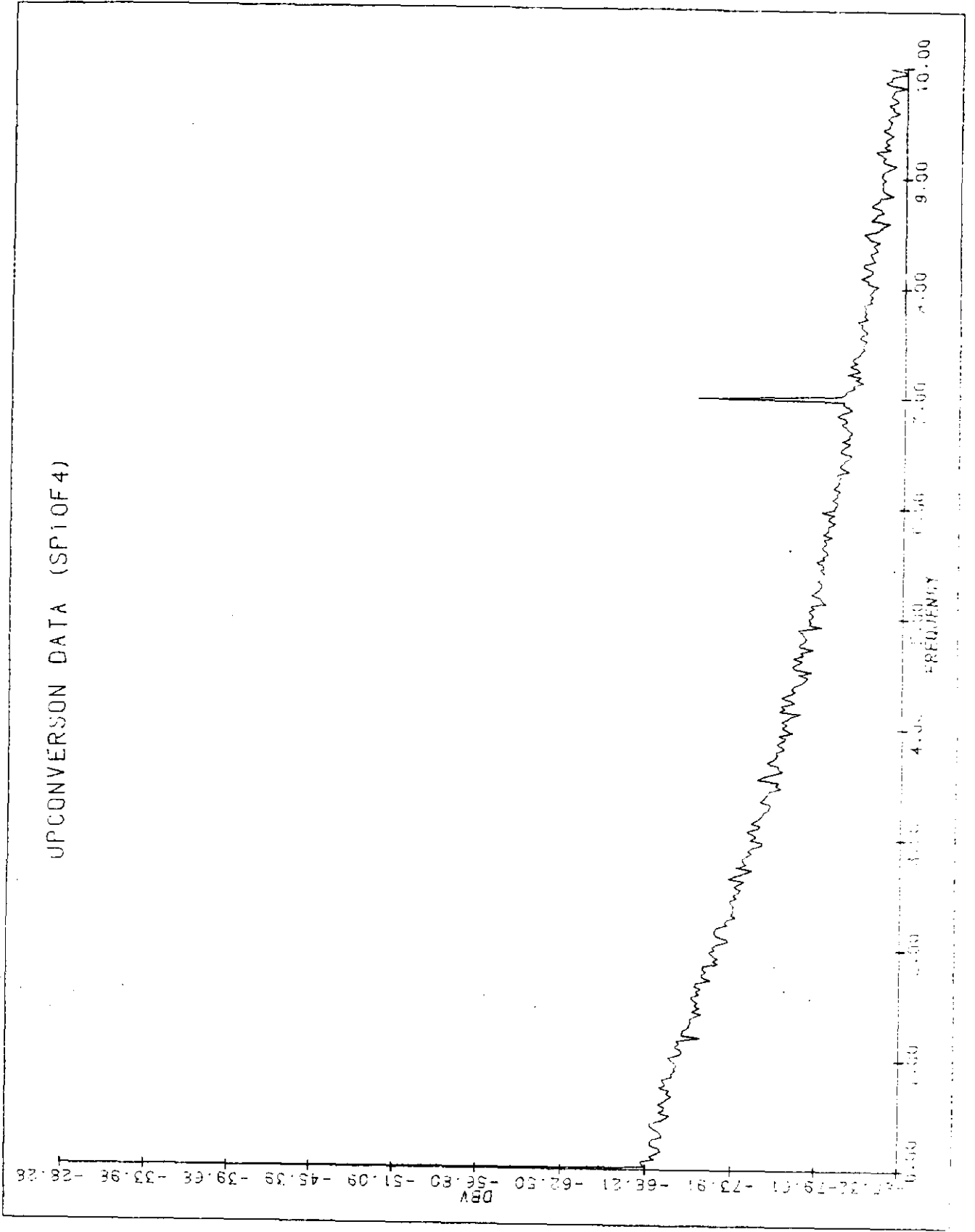


Figure 7b